Electronic Supplementary Material (ESI) for CrystEngComm.

Supplementary Materials

Chemical vapour synthesis of carbon nano-onions filled with high-spin ferromagnetic γ-$Fe_{50}Ni_{50}$ nanocrystals: a structural and magnetic investigation

Yini Liang [a], Aiqun Gu[b], Shanling Wang[b], Yi He[b], Shuping Zheng[b], Jian Guo[a]* and Filippo S. Boi[a]*

a. College of Physics, Sichuan University, Chengdu, China
b. Analytical and Testing Center, Sichuan University, Chengdu, China
Corresponding author: f.boi@scu.edu.cn, jianguo@scu.edu.cn

Instrumental Details

SEM acquisitions were obtained with a JSM-7500F at 15 kV. XRD with a Philips Xpert pro MPD (Cu K-α with λ = 0.154 nm). T-ESR with a JEOL JES-FA200 from T~77K to 300K, in the field range from 0 to 5000 G. TEM/HRTEM micrographs were acquired by employing a 200kV FEI Talos F200x and a 200 kV American FEI Tecnai F30. SQUID-magnetometry, with a MPMS-XL-5. XPS by employing a ThermoFisher, ESCALAB Xi+.

Supplementary Figures

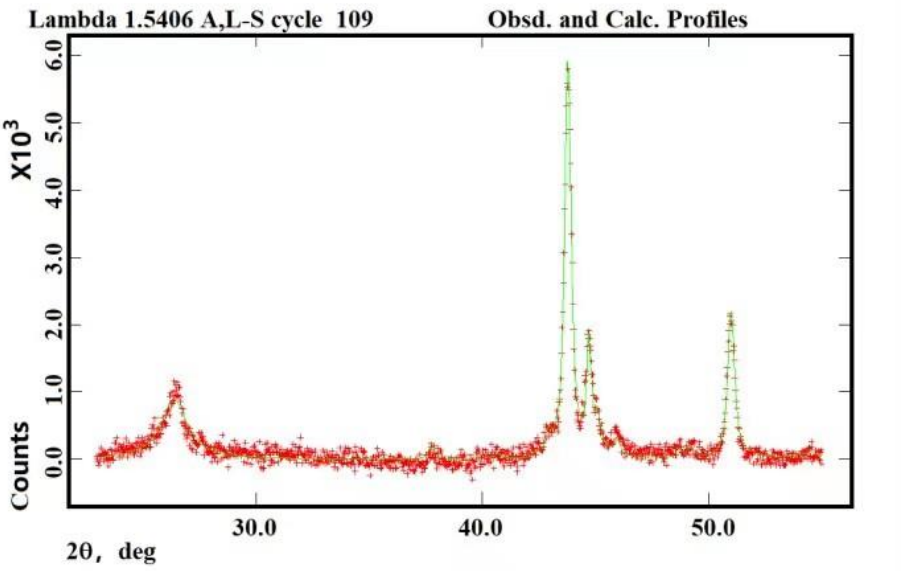

Figure S1: Typical XRD diffractogram (red crosses) and Rietveld refinement (green line) of the filled CNOs extracted from the region S1 of the reactor (method 1). The relative abundance of graphitic carbon extracted from the Rietveld was of ~ 57%.

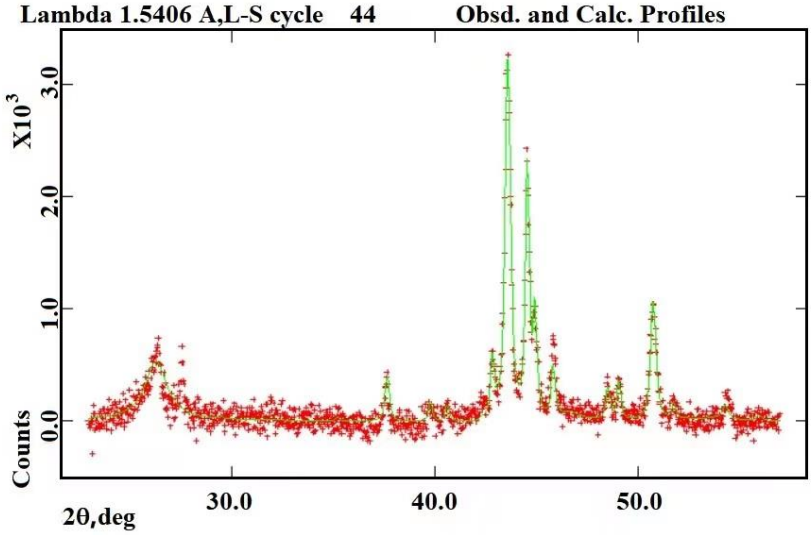

Figure S2: Typical XRD diffractogram (red crosses) and Rietveld refinement (green line) of the filled CNOs extracted from the region S2 of the reactor (method 1). The relative abundance of graphitic carbon extracted from the Rietveld was ~ 51%. Interestingly it is important to notice a significant enhancement in the relative quantity of Fe_3C (when compared to the S1 case), indicative of a higher content of interstitial carbon in the S2 region of the reactor. See main manuscript for Rietveld refinement analyses of the encapsulated crystals.

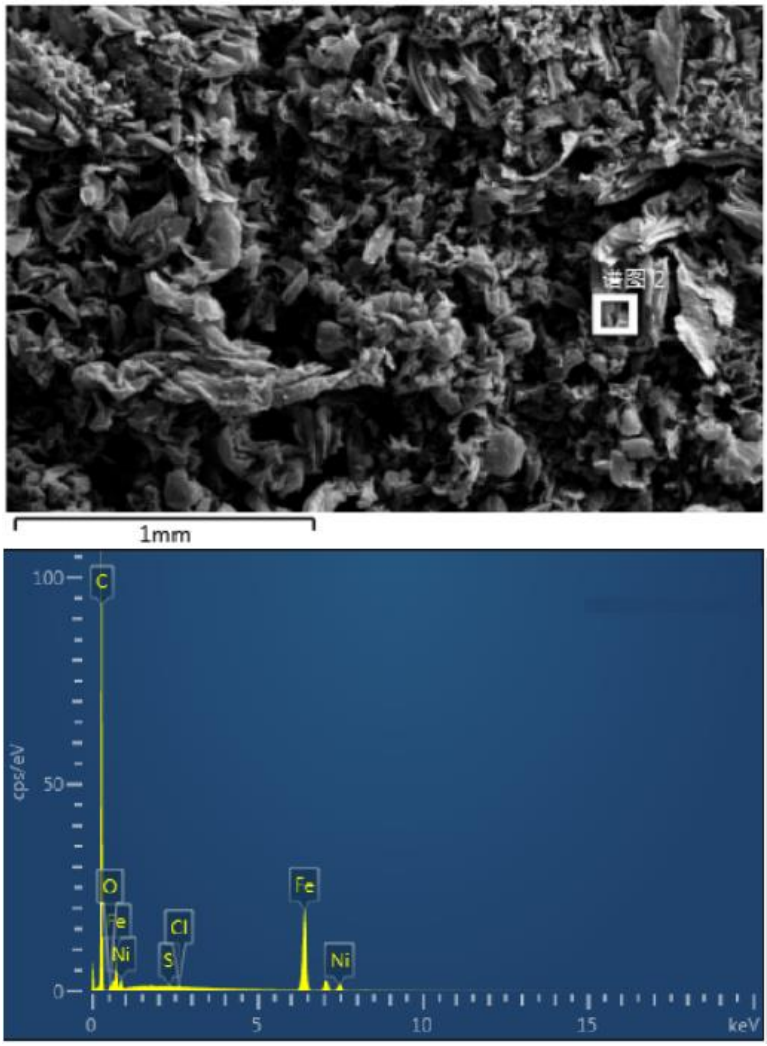

Element	Weight %	Atomic %
C	73.78	92.05
O	1.39	1.30
S	0.04	0.02
Cl	0.05	0.02
Fe	22.34	5.99
Ni	2.40	0.61

Figure S3: EDS analysis revealing the compositional characteristics of CNO film-flake located in the low Ni content zone of the S1 region (method 1). Note that the presence of Ni amounts in the order of 2.4% weight were reproducibly found in this deposition area.

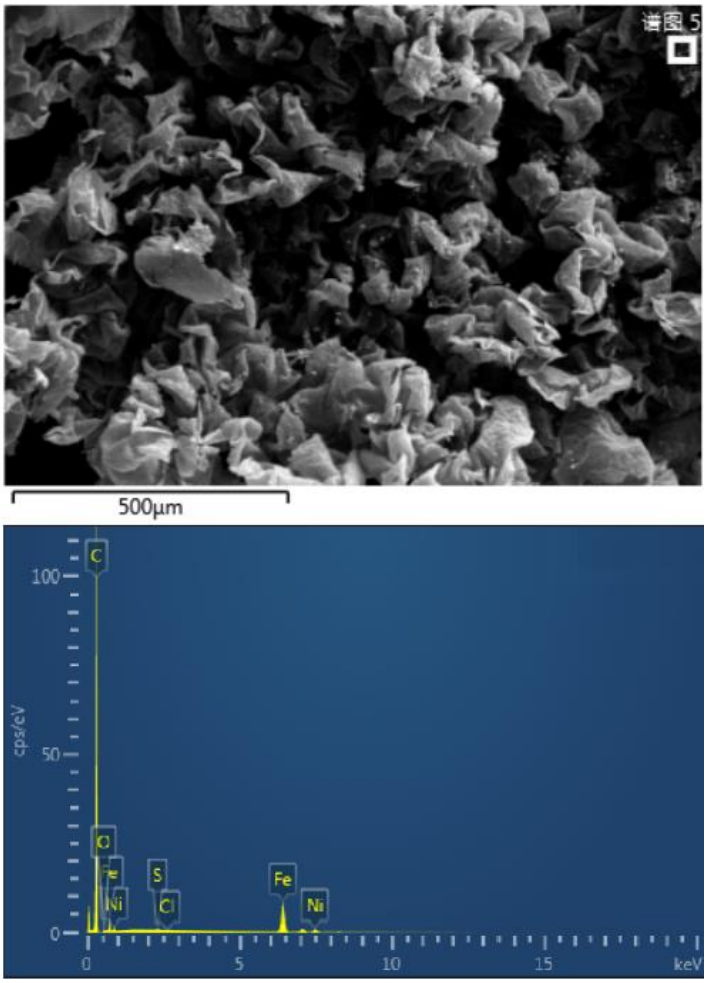

Element	Weight %	Atomic %
C	83.81	95.28
O	1.26	1.08
S	0.09	0.04
Cl	0.03	0.01
Fe	12.56	3.07
Ni	2.24	0.52

Figure S4: Additional EDS analysis revealing the compositional characteristics of CNO film-flake located in the low Ni % content zone of the S1 region (method 1). Note the presence of Ni amounts in the order of 2.2% weight.

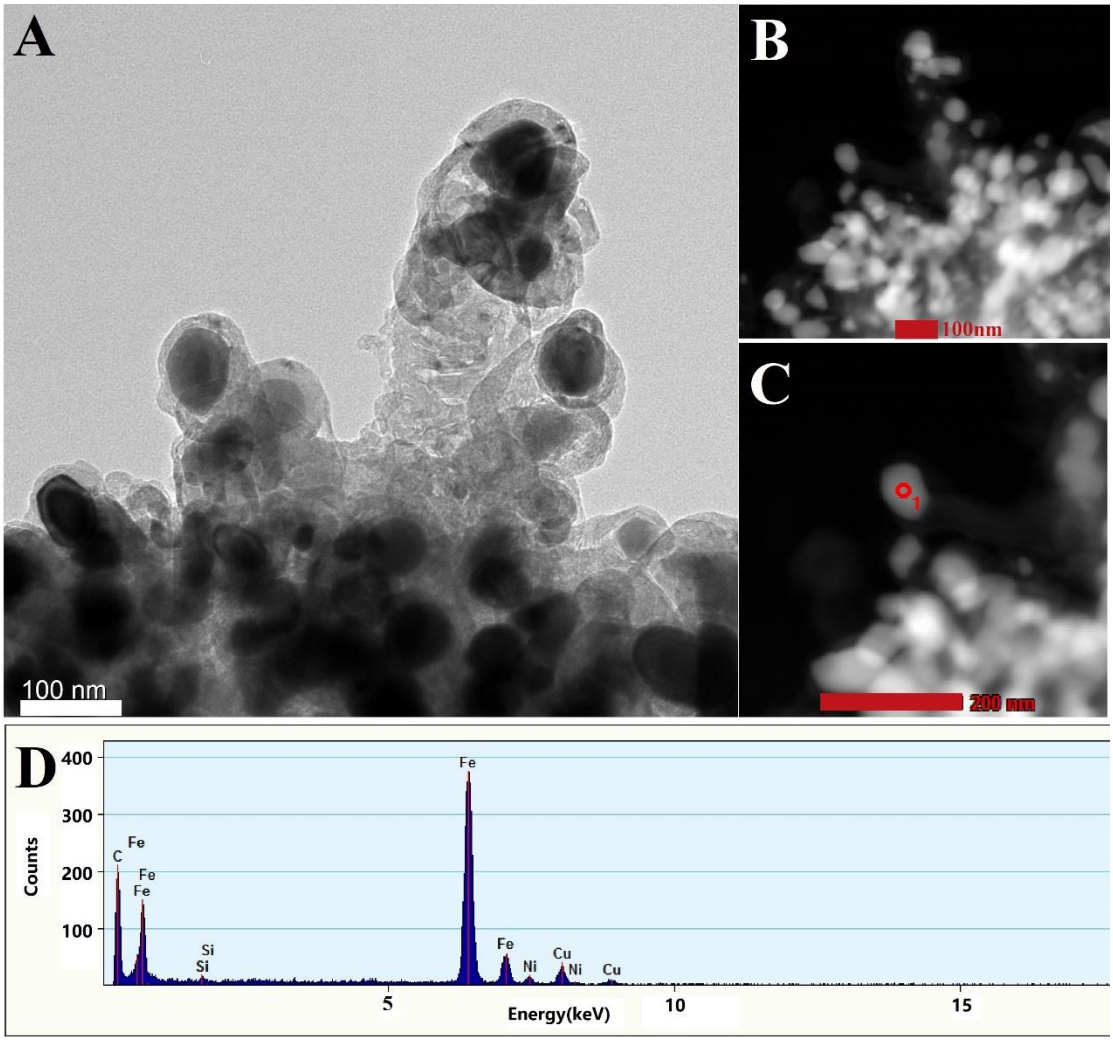

Element	Weight %	Atomic %	Uncert %	Detector Correction	k-Factor
C (K)	39.98	75.63	1.00	0.26	3.940
Fe (K)	57.35	23.33	0.65	0.99	1.403
Ni (K)	2.65	1.02	0.14	0.99	1.511

Figure S5: TEM (A), STEM (B,C) /EDS (D) of typical filled CNOs extracted from the low Ni % content region of the S1 deposition area. A quantity of ~2.6 weight % of Ni was found in the EDS analyses.

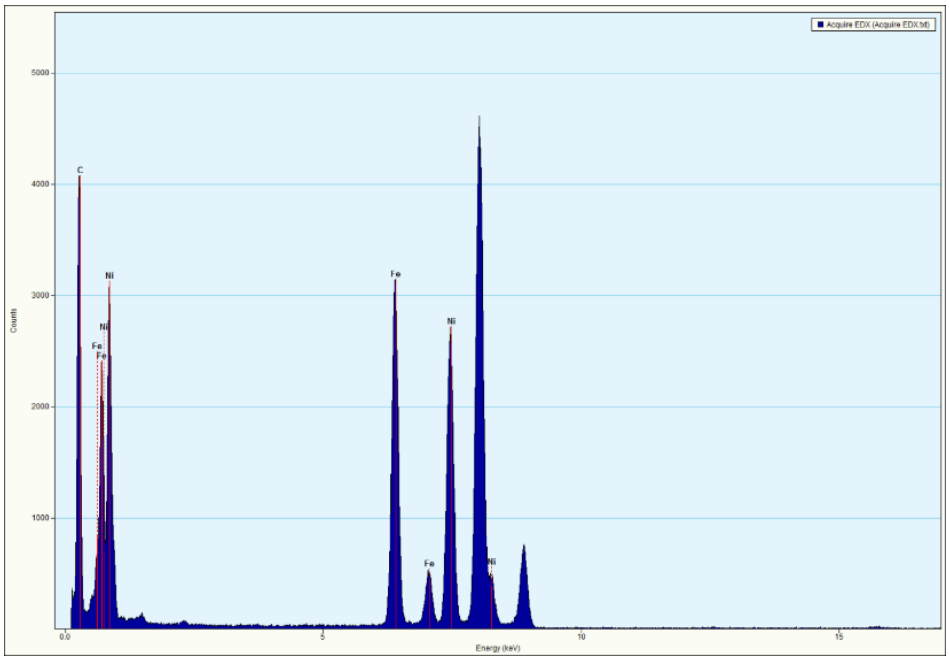

Element	Weight %	Atomic %
C(K)	42.26	77.71
Fe(K)	29.39	11.62
Ni(K)	28.34	10.66

Figure S6: EDS analysis (see table for weight % and atomic % values) of a CNO obtained with the method 1, by pyrolysis of ferrocene, nickelocene, dichlorobenzene and sulfur mixtures in the region S1 (high Ni content region) of the reactor (see Fig.2B and Fig.1).

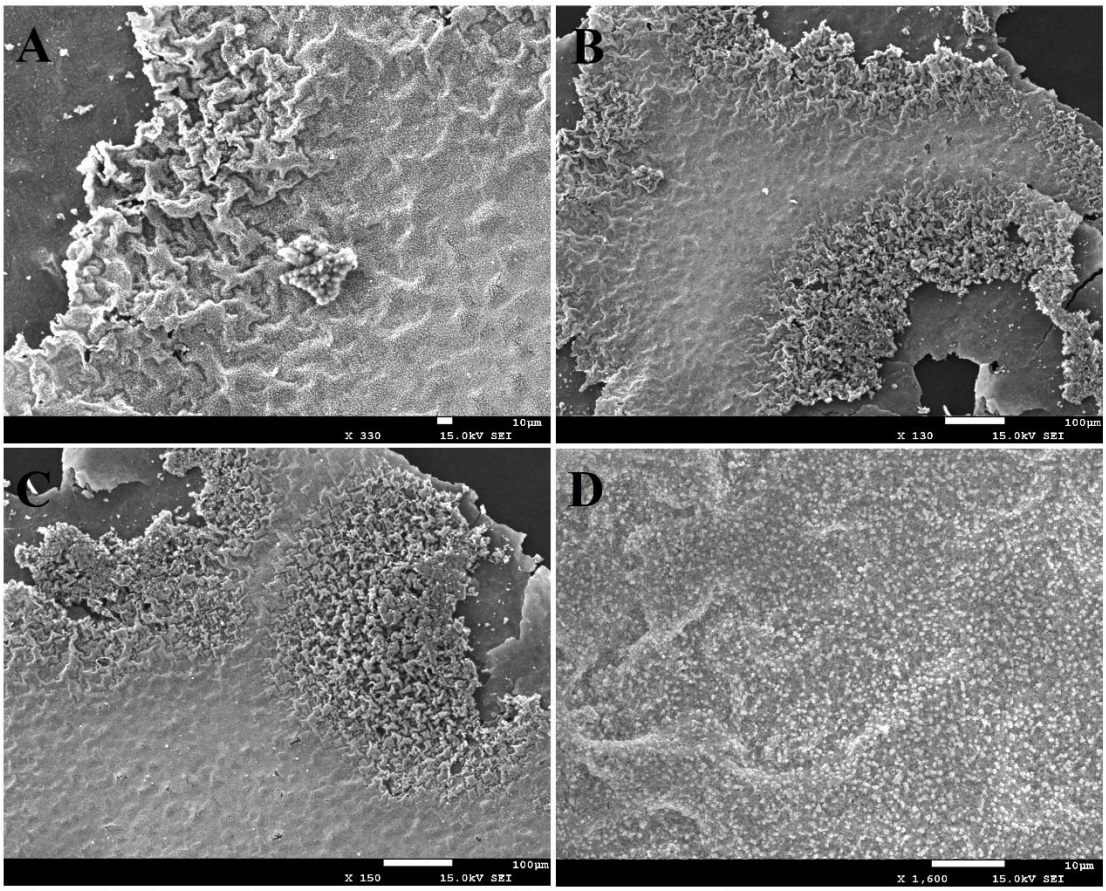

Figure S7: SEM characterization of the filled CNOs obtained with the method 1 by pyrolysis of a ferrocene, nickelocene, dichlorobenzene and sulfur mixtures in the S1 region of the reactor (high Ni % content region, see schematic in Fig.1).

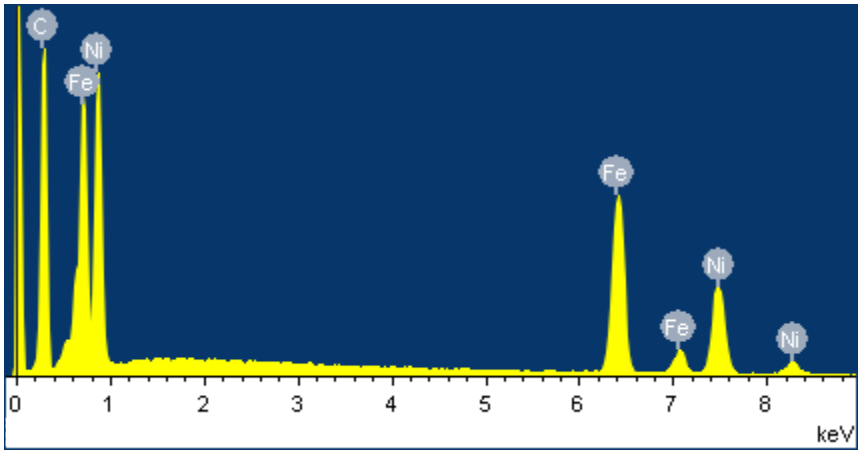

Element	Weight %	Atomic %
C (K)	42.92	78.17
Fe (K)	29.69	11.63
Ni (K)	27.39	10.21

Figure S8: EDS analyses revealing the compositional properties of the CNOs grown in the area S1 (high Ni content region, see Fig.1) of the reactor (method-1).

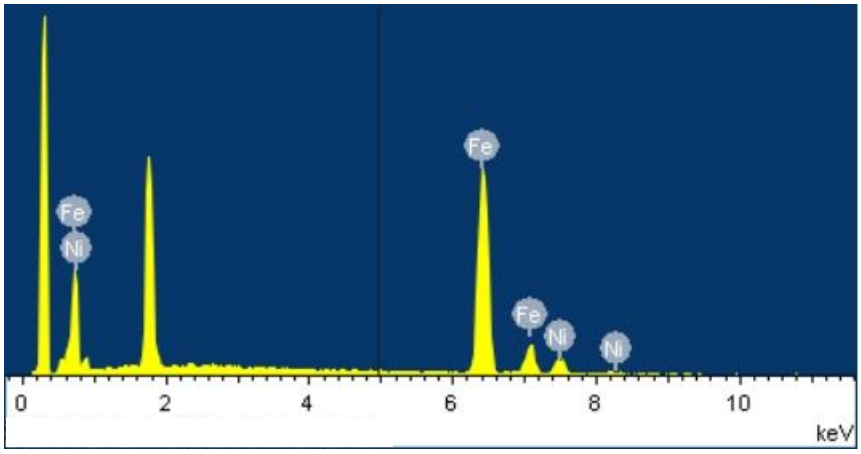

Element	Weight %	Atomic %
Fe (K)	89.47	89.93
Ni (K)	10.53	10.07

Figure S9: EDS analyses revealing the compositional properties of the CNOs grown in the area S2 of the reactor (Fig.1, main manuscript). Note the significant depletion in Ni content (method-1). The unlabeled peak arises from the Si-substrate.

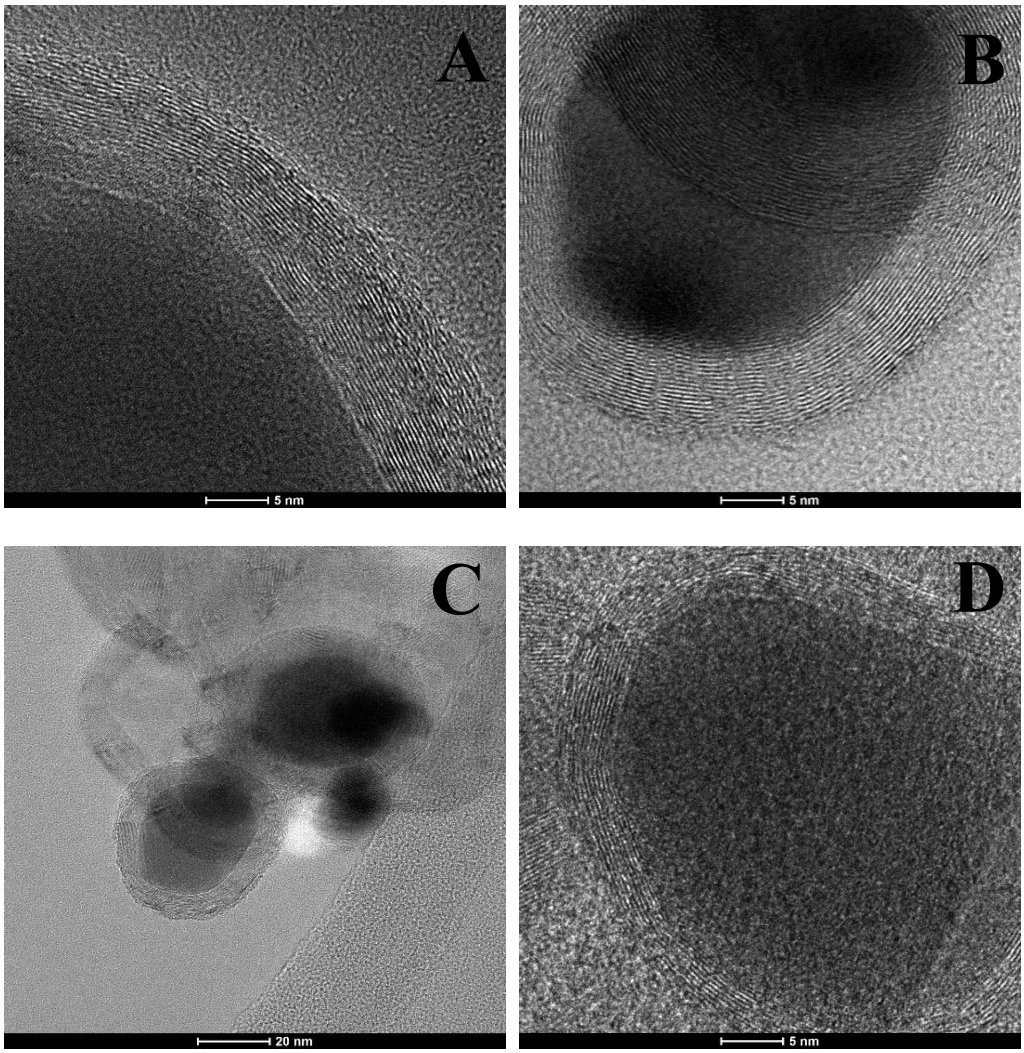

Figure S10: Transmission electron micrographs revealing the cross-sectional morphology of the filled CNOs grown in the region S1 of the reactor (method-1, high Ni% content region). In A-C different views of the same nano-onion, exhibiting the presence of a multilayered graphitic structure. In D an additional example, exhibiting the graphitic ordering of the CNO layers.

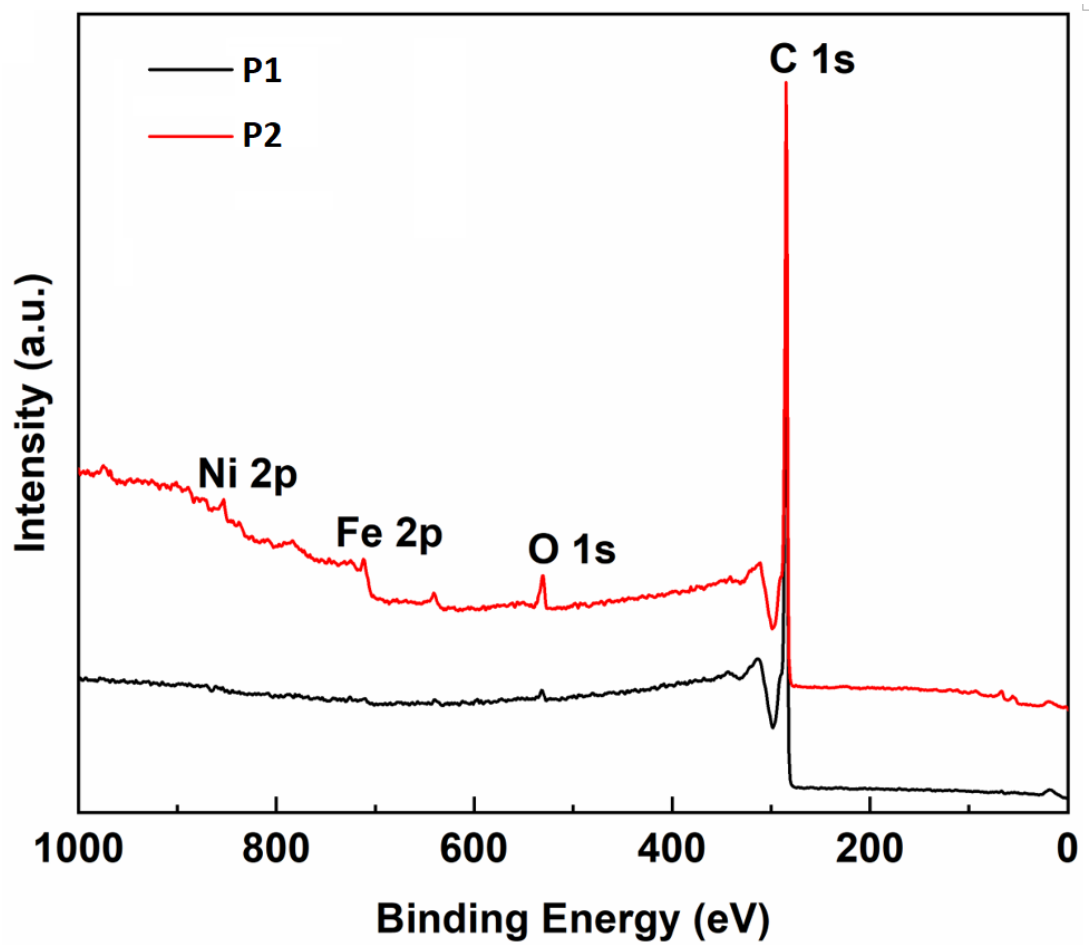

CNOs S1	C (atom%)	Fe (atom%)	Ni (atom%)
P1	99.40	0.32	0.28
P2	97.65	1.49	0.86

Figure S11: XPS point-acquisition analyses and survey spectra evidencing the presence of Fe and Ni components in two points of the as grown filled CNO film (method-1, S1). It is worth noting that the actual Fe and Ni content in the sample may not match with the data in the table due to the formation of metal/alloy-core and carbon-shell (multilayered CNOs) structures.

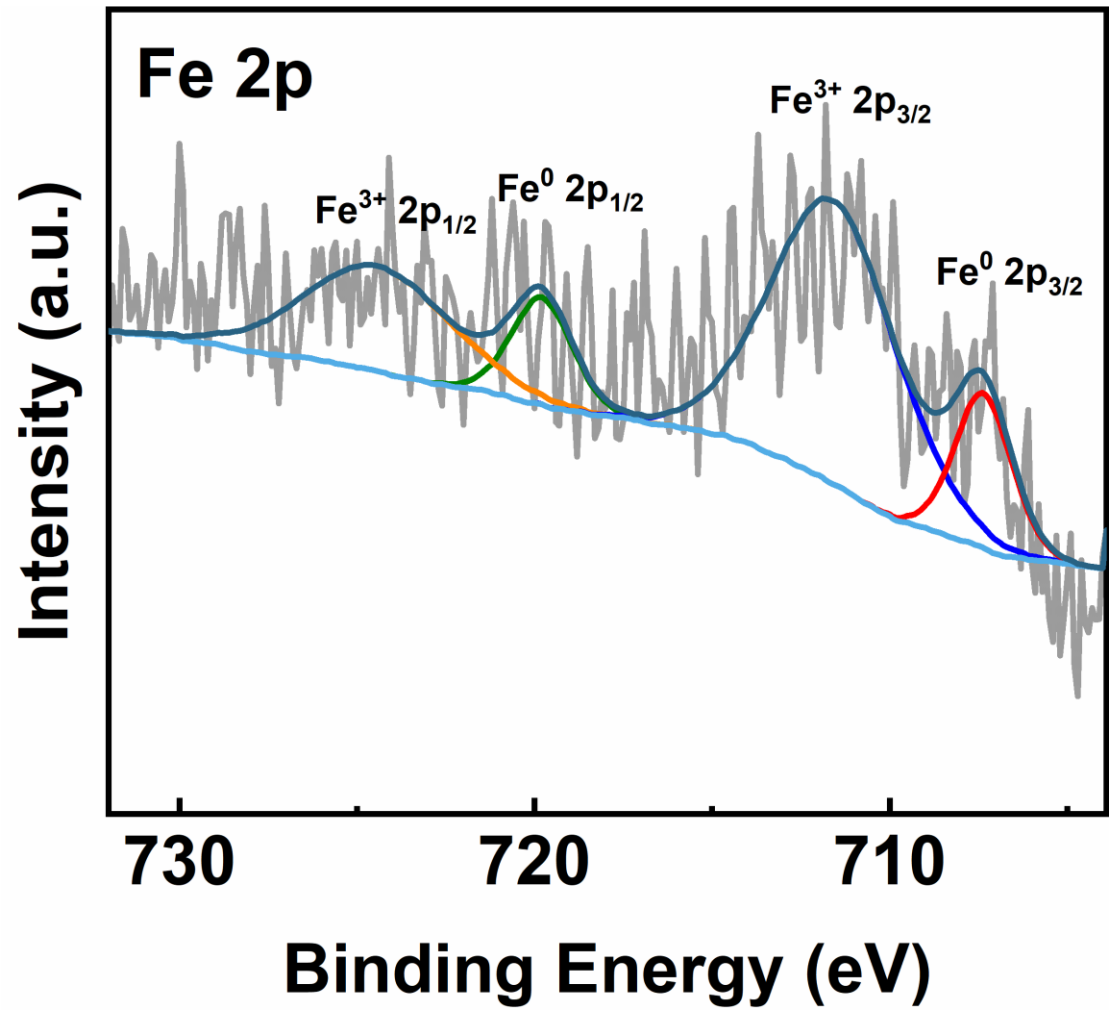

Figure S12: High detail XPS signal obtained from the sample S1(method-1) and respective deconvolution analyses. Note the presence of contributions arising from Fe^{3+} and Fe^{0} components. The observation of Fe^{3+} components suggest the existence of contribution-traces from surface oxidation.

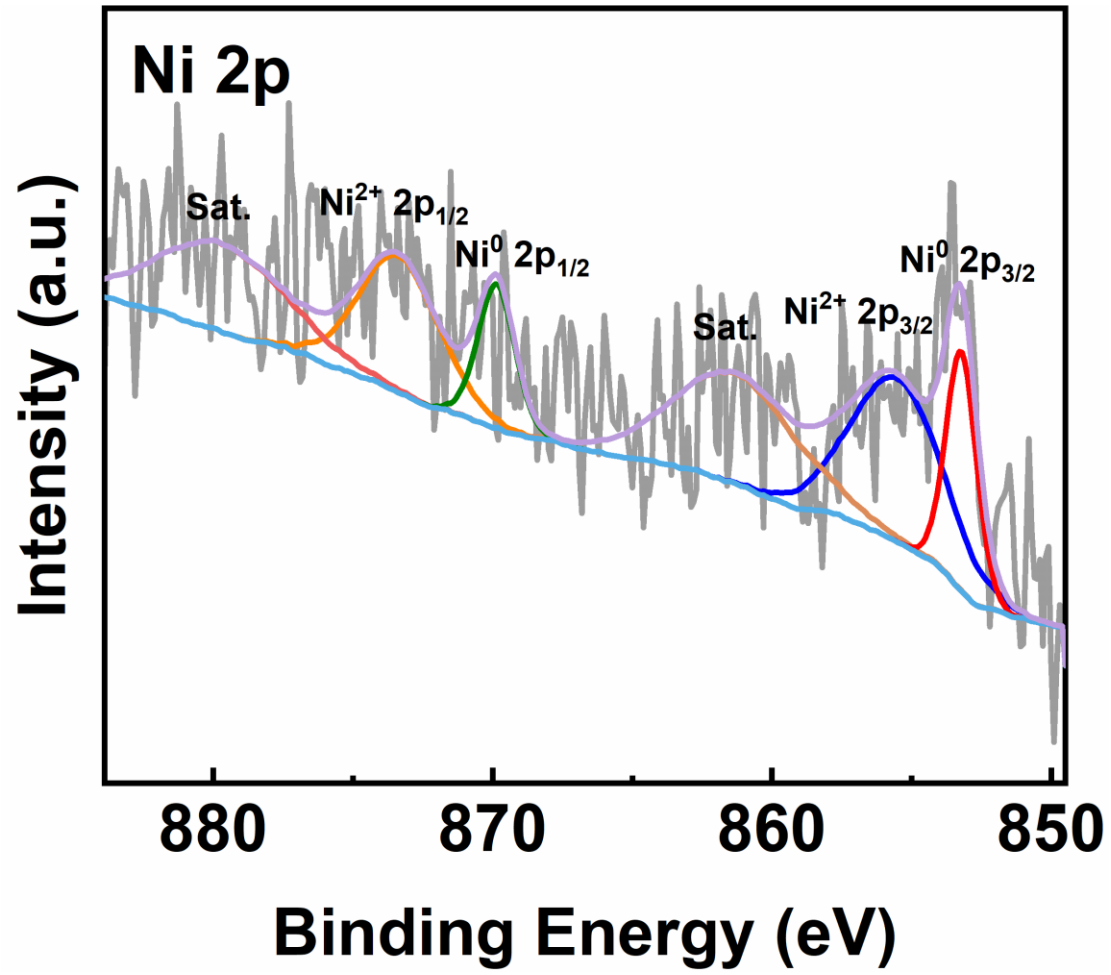

Figure S13: High detail XPS signal obtained from the sample S1(method-1) and respective deconvolution analyses. Note the presence of contributions arising from Ni^{2+} and Ni^{0} components. The presence of Ni^{2+} components suggests the existence of traces of NiO due to surface oxidation.

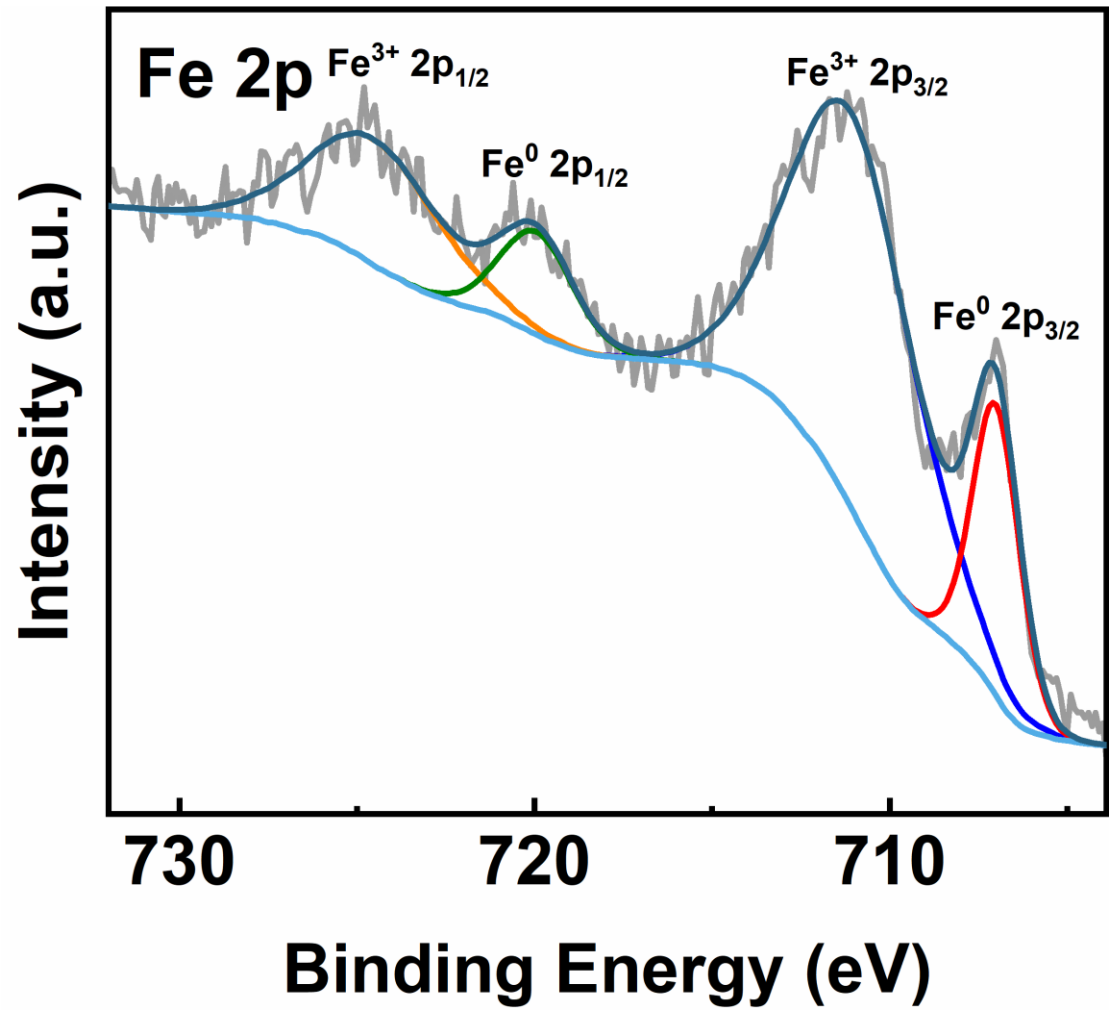

Figure S14: High detail XPS signal obtained from another point region of the substrate (method-1) and respective deconvolution analyses. Note the presence of contributions arising from Fe^{3+} (surface oxidation) and Fe^{0} (metallic iron) components.

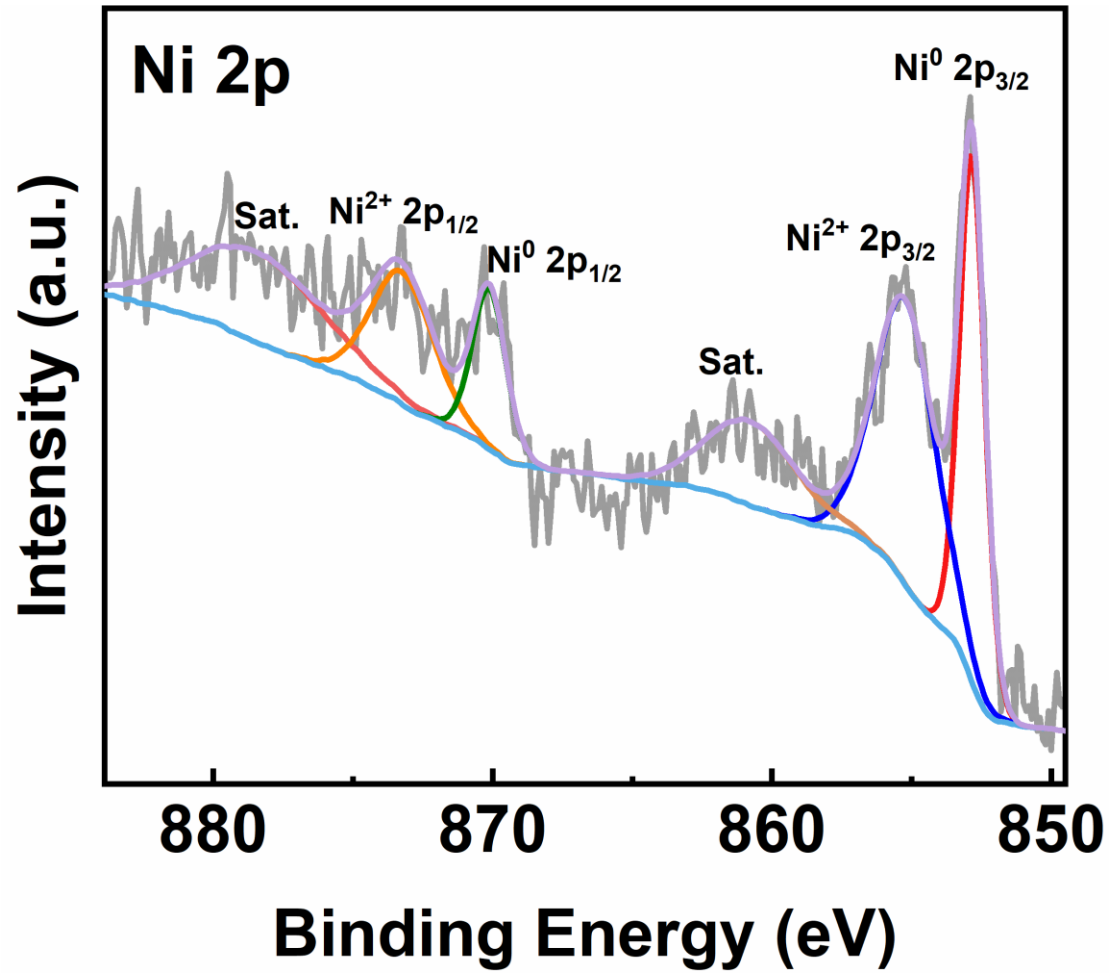

Figure S15: High detail XPS signal obtained from another point region of the substrate (method-1, S1 region) and respective deconvolution analyses. Note also in this case the presence of contributions arising from $Ni^{2+}$and Ni^{0} components.

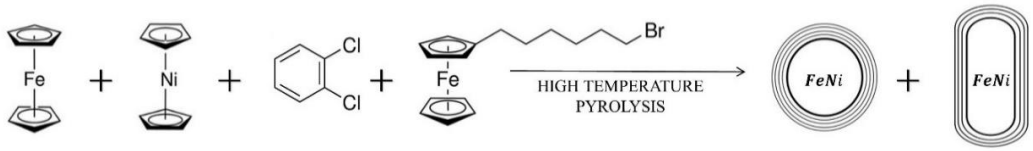

Figure S16: Schematic diagram of the modified chemical vapour synthesis (method-2), in which 60 mg of ferrocene, 10 mg of nickelocene, 0.05 mL of dichlorobenzene and ~ 0.05 mL of (6-bromohexyl) ferrocene were pyrolyzed at T~ 990°C. Noticeably, the resulting synthesis product was found to consist of mixtures of CNOs and CNTs.

Br-assisted method 2 TEM

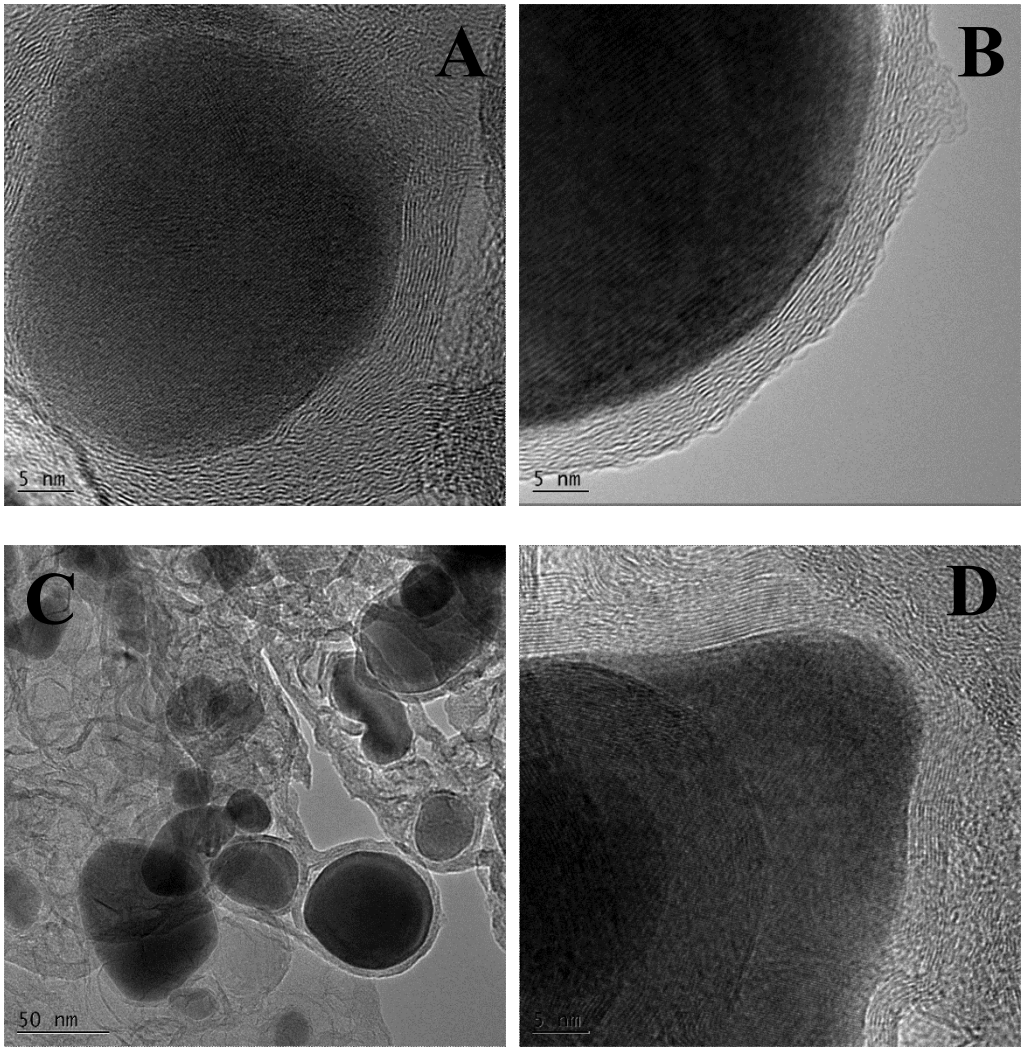

Figure S17: Transmission electron micrograph showing the morphology of the CNOs obtained by pyrolysis of ferrocene, nickelocene, dichlorobenzene with (6-bromohexyl) ferrocene, in absence of sulfur.

Br-assisted Method2- S1 XRD

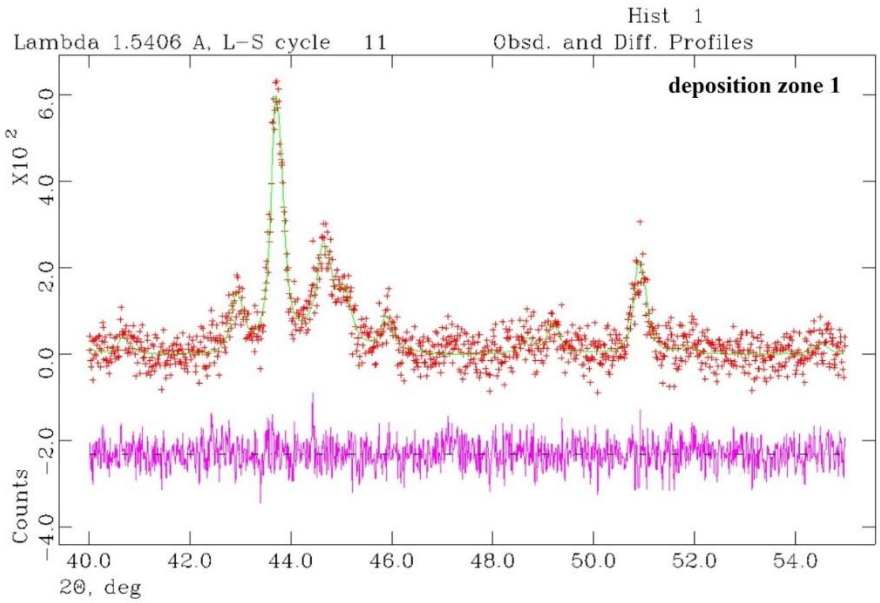

Figure S18: XRD diffractogram (red crosses) and Rietveld refinement analysis (green line) of the CNOs obtained with the method-2, in the zone S1 of the reactor. The extracted relative abundances were 11.75% of α-Fe, 48.37% of Fe_3C, 39.8% of γ-$Fe_{70}Ni_{30}$.

Br-assisted Method2-S2 XRD

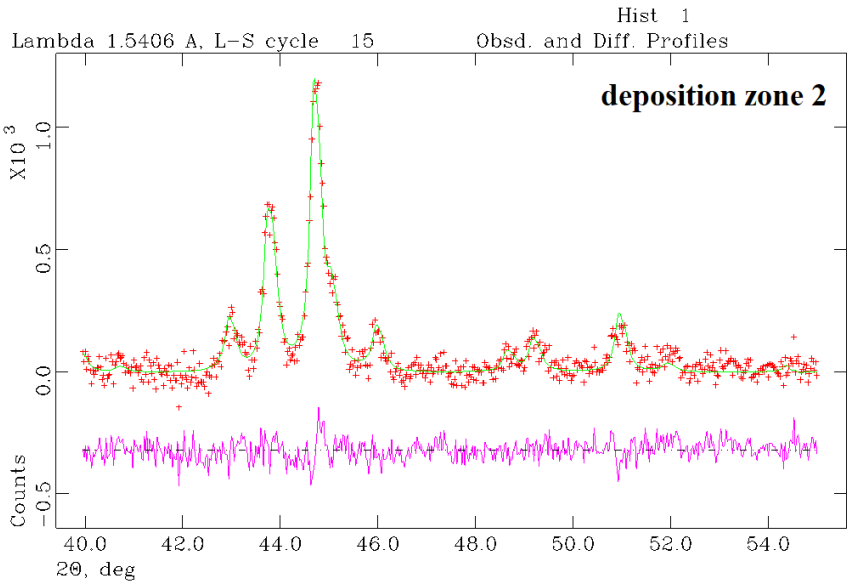

Figure S19: XRD diffractogram (red crosses) and Rietveld refinement analysis (green line) of the CNOs obtained with the method-2, in the zone S2 of the reactor. The extracted relative abundances were 42.57% of Fe_3C, 37.9% of α-Fe, 19.48% of γ-Fe.

Br-assisted method 2 SEM

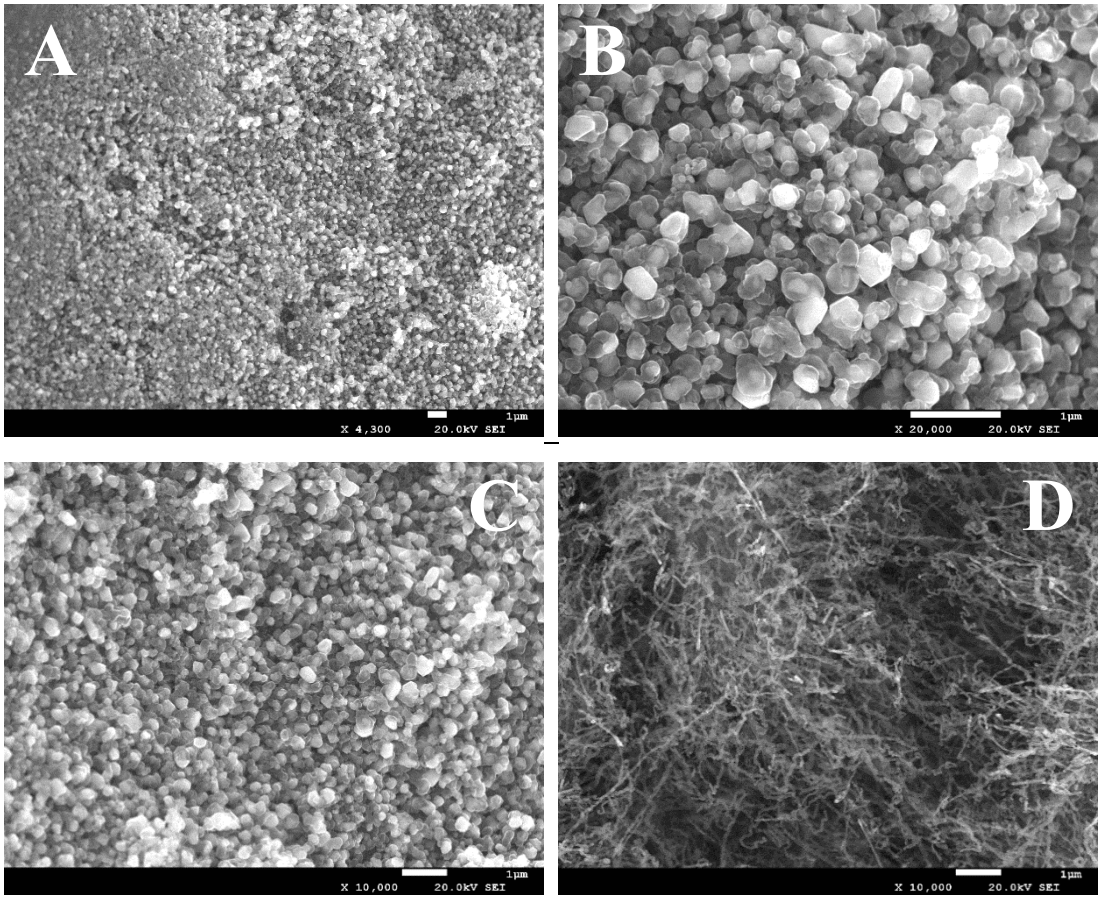

Figure S20: SEM characterization of filled CNOs (A-C)/CNTs (D) obtained by pyrolysis of mixtures containing ferrocene, nickelocene, dichlorobenzene and (6-bromohexyl) ferrocene.

Br-S1 SEM EDS

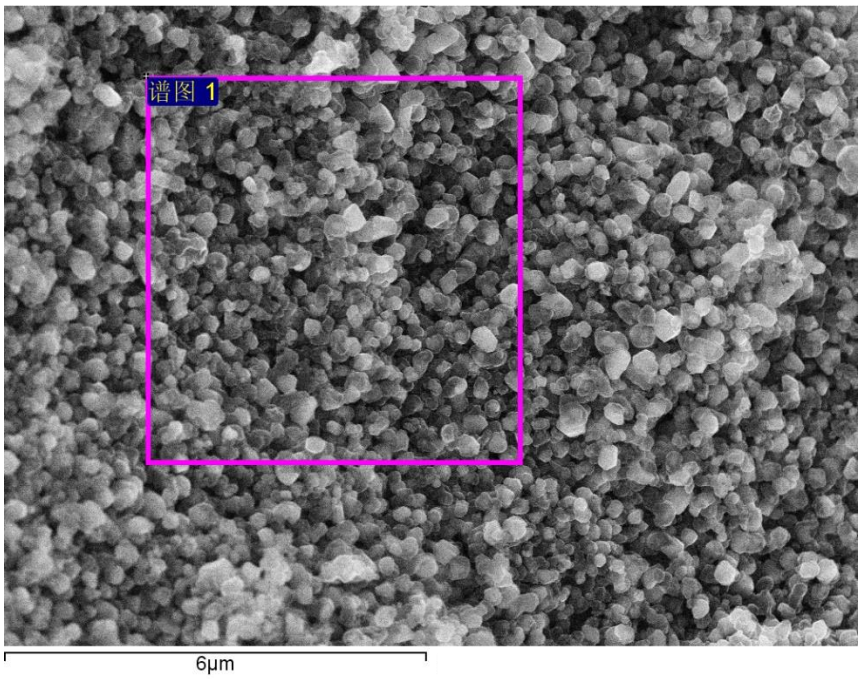

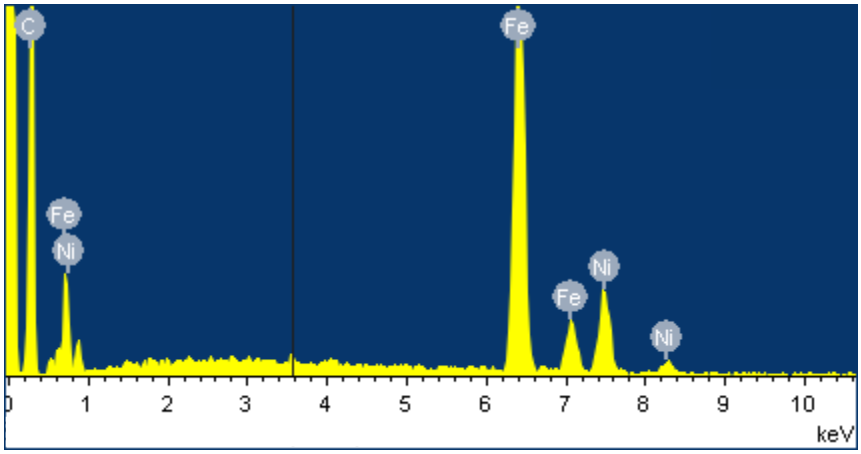

Element	Weight %	Atomic %
C（K）	57.02	86.19
Fe（K）	32.75	10.65
Ni（K）	10.23	3.16

Figure S21: SEM and EDS analyses of the filled CNOs obtained by pyrolysis of precursor mixtures containing ferrocene, nickelocene, dichlorobenzene and (6-bromo hexyl) ferrocene in the deposition zone 1 of the reactor (S1,method-2).

Br-S2 SEM EDS

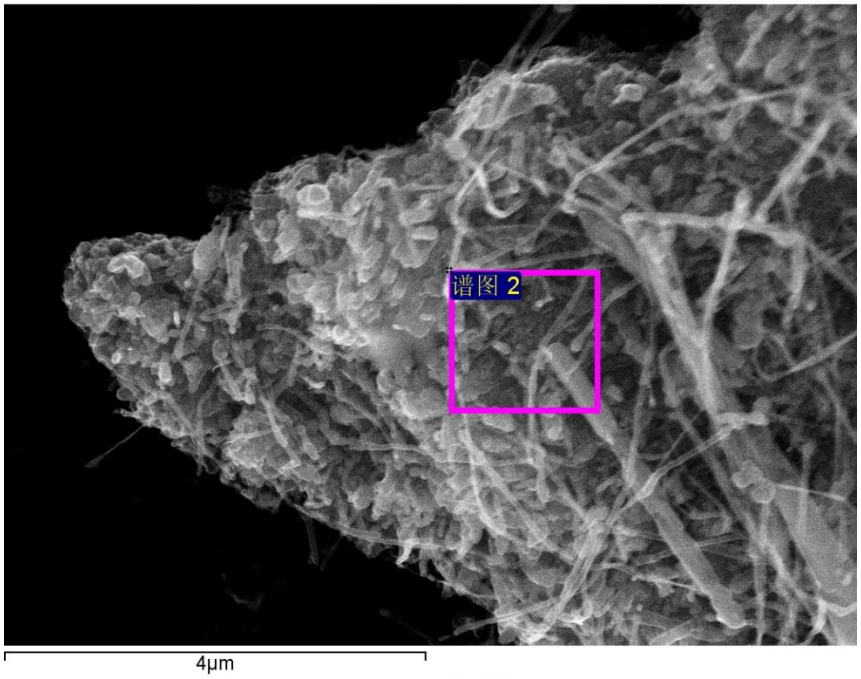

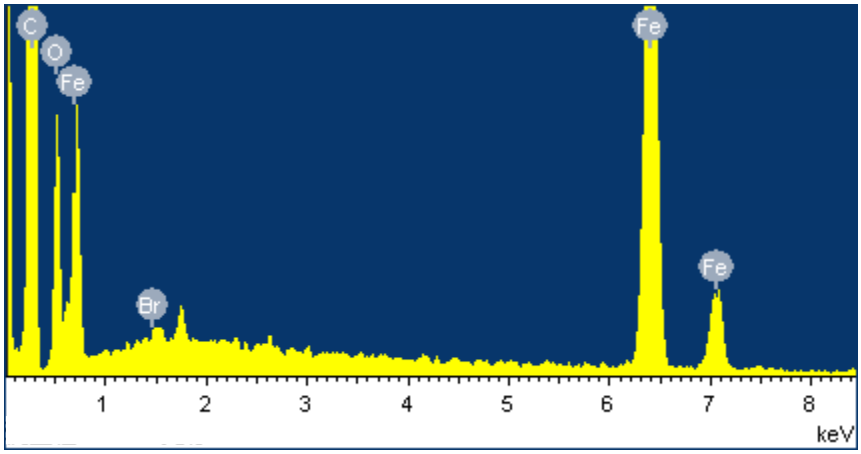

Element	Weight %	Atomic %
C (K)	70.89	84.41
O (K)	12.78	11.42
Fe (K)	16.16	4.14
Br (L)	0.17	0.03

Figure S22: SEM and EDS analyses of the filled CNOs/CNTs obtained by pyrolysis of precursor mixtures containing ferrocene, nickelocene, dichlorobenzene and (6-bromohexyl) ferrocene in the deposition zone 2 of the reactor (S2, method-2). Note the vanishing of Ni content in the second deposition zone of the reactor.

Br-S1 XPS

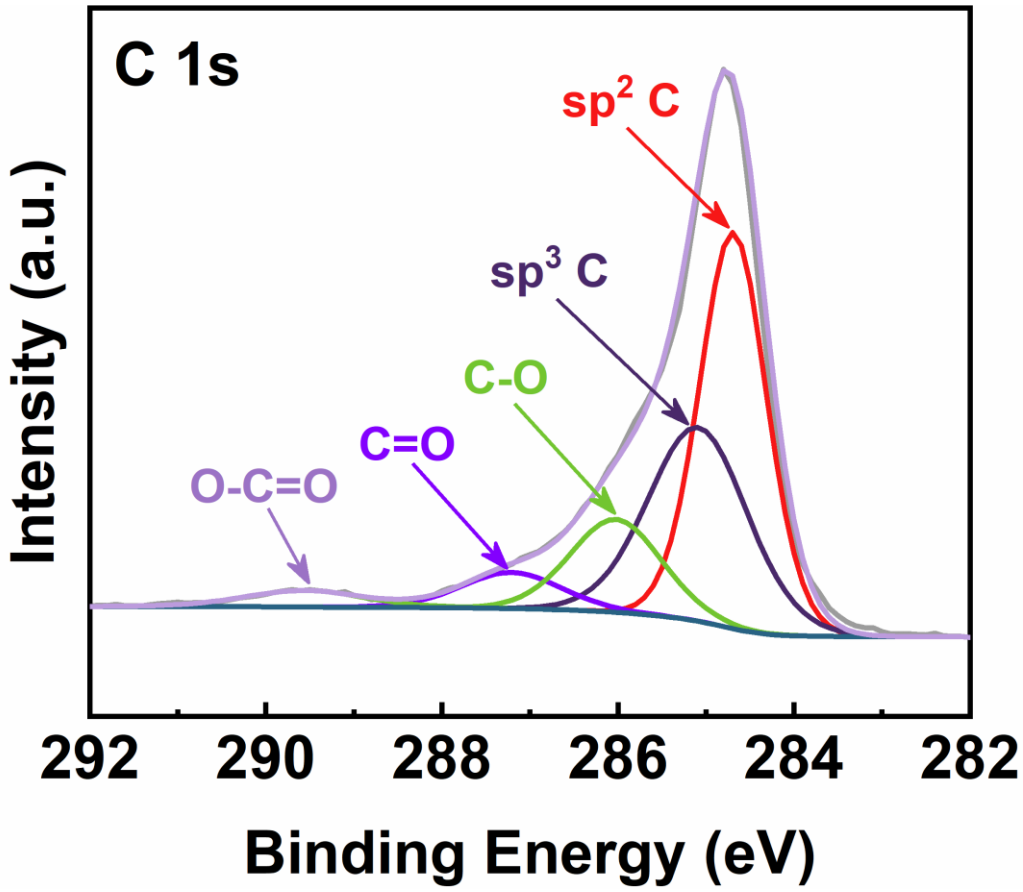

Figure S23: Typical XPS acquisition of the C1s spectrum from a carbon nano-onion sample obtained with the method 2 (deposition zone 1) revealing the following relative abundances of carbon bonding features: sp^2 C (44.39%), sp^3 C (32.17%), C-O (14.18%), C=O (6.01%) and O-C=O (3.25%),